

# EVALUATION OF GPM-ERA CONSTELLATION PRECIPITATION ESTIMATES FOR LAND SURFACE MODELING APPLICATIONS

F. Joseph Turk<sup>1</sup>, G. Mostovoy<sup>2</sup>, V. Anantharaj<sup>2</sup>, P. Houser<sup>3</sup>, QiQi Lu<sup>4</sup>, Y. Ling<sup>2</sup>

<sup>1</sup>Naval Research Laboratory, Marine Meteorology Division, Monterey, CA 93943 USA

<sup>2</sup>GeoResources Institute, Mississippi State University, Starkville, MS 39762 USA

<sup>3</sup>Center for Research on Environment and Water, George Mason University, VA USA

<sup>4</sup>Dept. of Mathematics and Statistics, Mississippi State University, Starkville, MS USA

## Abstract

The Global Precipitation Mission (GPM) is a joint mission between the National Aeronautics and Space Agency (NASA) and the Japanese Aerospace Exploration Agency (JAXA). It builds upon the heritage of the Tropical Rainfall Measuring Mission (TRMM) with an advanced core spacecraft augmented by a constellation satellite and other satellites of opportunity (i.e., other international satellite systems with precipitation-sensing instrument payloads). With changes to satellite missions and sensor capabilities, it is unlikely that the GPM constellation configuration will be known until close to deployment, and will change during the lifetime of GPM. It is instructive to note how the retention or loss of a particular satellite platform and/or sensor type will affect the performance of the GPM precipitation products and other applications that utilize GPM products. In this study, we use the existing (2008) constellation of various active radar and passive microwave-based platforms to examine the impact of several proxy GPM satellite constellation configurations. The emphasis is on how high resolution precipitation products (HRPP) are affected by such factors as sensor type (conical or across-track scanning) and nodal crossing time, using a collection of GPM proxy datasets gathered over the continental United States. The validation is presented two ways. The first is by traditional validation using an existing surface gauge network analysis (Chen et. al, 2008). The second is more indirect, through examination of how the soil moisture state of the Noah land surface model (LSM) is impacted when the LSM is forced with the various precipitation datasets, each corresponding to a different proxy GPM constellation configuration.

## HIGH RESOLUTION PRECIPITATION PRODUCTS (HRPP)

High Resolution Precipitation Products (HRPP) combine a multitude of spaceborne remotely-estimated and ground-based datasets in order to generate a precipitation product that is of a finer spatial and/or temporal resolution than any of the individual input datasets. These HRPPs are relevant to a variety of applications relating to Earth's hydrological cycle. Passive microwave sensors onboard low Earth orbiting (LEO) and geostationary Earth orbiting (GEO) environmental satellite systems provide the basic building blocks of an HRPP, augmented in some cases by surface radar and raingauge information and analyses from numerical weather prediction (NWP) models. Examples of commonly used HRPPs are the Global Precipitation Climatology Program (GPCP) one-degree daily (1DD) combined precipitation data set (Huffman et. al, 2001), the Precipitation Estimation from Remotely Sensed Information using Artificial Neural Networks (PERSIANN) datasets (Hsu et. al, 1997), the Climate Prediction Center morphing technique (CMORPH) (Joyce et. al, 2004), and the NRL-Blend (Turk and Miller, 2006), among others. Typically, these HRPPs combine multiple satellite datasets (and some add in additional raingauge and other non-satellite data) and produce estimates of three-hourly accumulated precipitation between  $\pm 60$  degrees latitude, updated every three hours, at a gridded spatial resolution of 0.25-degrees. From these three-hourly accumulations, longer time scale accumulations can be generated. Some of these HRPPs are designed to be operated strictly in near realtime (e.g., NRL-Blend), while others create near realtime as well as a higher quality, post-processed non-realtime datasets.

An example of one HRPP (the NRL-Blend product) is shown in Figure 1a. In this figure, the 12-hour precipitation accumulations ending at 12 UTC on 6 September 2006 are shown (color scale in units of mm), with the grayshade background depicting a composited longwave infrared (IR) satellite image at the accumulations end time. Visually, the depiction and location of precipitation appears consistent with known precipitation patterns at this time of year, e.g., several tropical cyclones in the Atlantic Ocean and tropical disturbances in the western Pacific Ocean. However, associated with each pixel is an error whose structure has many components. For example, the majority of the error is likely associated with the accumulated errors from the instantaneous rainrate estimates provided by each component satellite. Other error may be from precipitation evolution that was not captured by the intermittent revisit schedule of the component satellites.

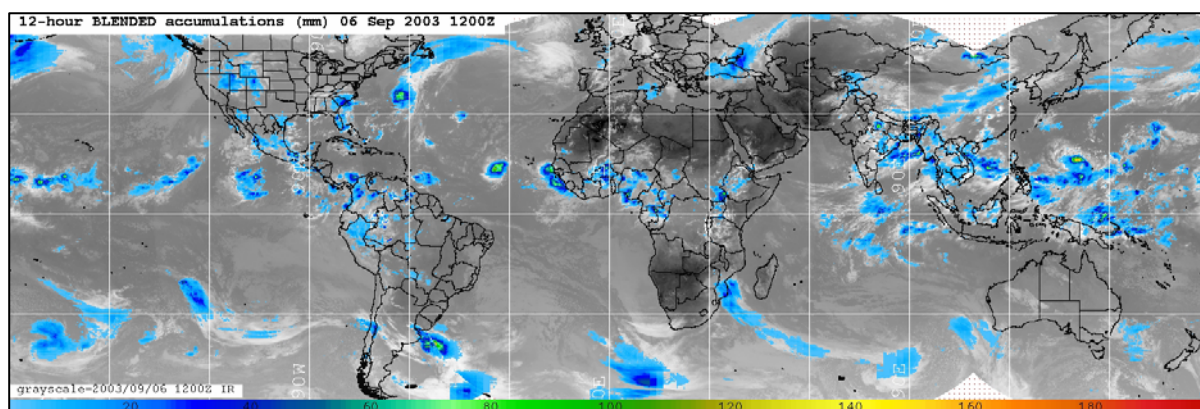


**Figure 1a.** 12-hour accumulated precipitation (color scale in mm) ending at 12 UTC on 6 September 2006 from the NRL-Blend HRPP.

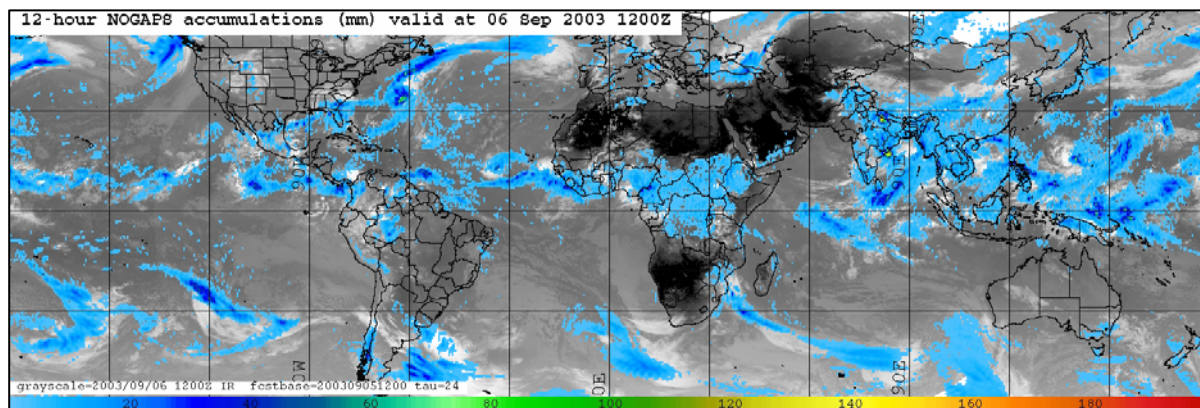


**Figure 1b.** As in Figure 1a, but the 12-hour accumulated precipitation (color scale in mm) ending at 12 UTC on 6 September 2006 from the 24-hour forecast of the NOGAPS model.

An additional source of global precipitation data is available from many global numerical weather prediction (NWP) forecast models. While many NWP models do not yet specifically carry rain as a prognostic variable, the conversion of cloud liquid water to rain is typically based on various temperature and humidity thresholds, including parameterizations of convective processes. Since models evolve the moisture with the dynamical state of the atmosphere, the models generally do a better job of following the movement of precipitation associated with frontal systems. The motion-based HRPPs such as CMORPH tend to perform better than other types of HRPPs which have no knowledge of the atmospheric dynamical state. Although an NWP model precipitation dataset is a forecast and not a true observation, it nevertheless is an additional source of data that in some cases

may outperform the HRPPs. An example from the Navy Operational Global Atmospheric Prediction System (NOGAPS) NWP forecast model is shown in Figure 1b, valid at the same time as Figure 1a. While NOGAPS does capture the same basic patterns of precipitation as noted in Figure 1a, there are regions of discrepancy. For example, the model tends to spread out too much light precipitation and doesn't capture the intense, smaller scale precipitation (e.g, tropical cyclones). On the other hand, the model pick up light rain associated with mid-latitude frontal systems and doesn't show evidence of discontinuities between land and water backgrounds (which is an issue with passive-microwave based precipitation estimates).

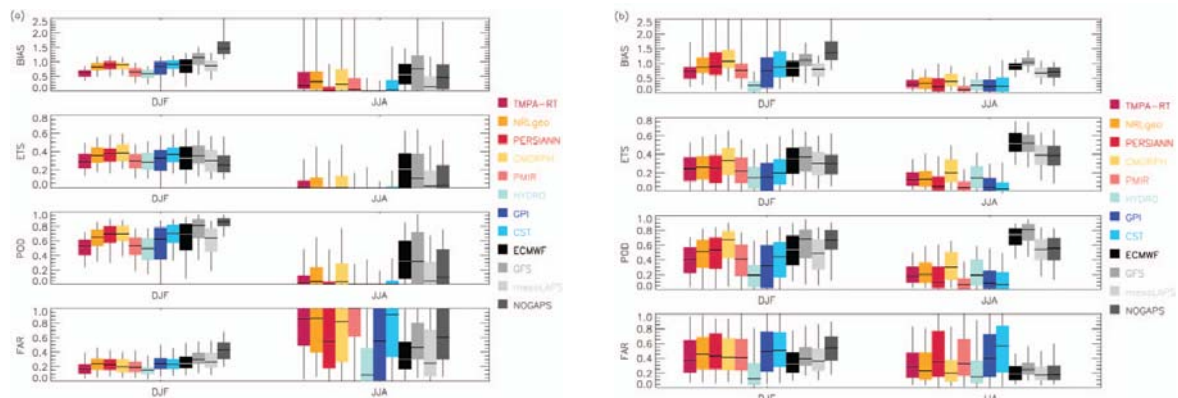


**Figure 2.** Seasonal performance of precipitation datasets over continental Australia north of 30S latitude (left) and south of 30S latitude (right), using a threshold of  $1 \text{ mm day}^{-1}$ . From top, bias, equitable threat score (ETS), probability of detection (POD) and false alarm rate (FAR) from eight satellite-based HRPPs (colored boxes) and four NWP models (grayshade boxes).

In order to find their widest usage and impact, the specification of the error structure of each HRPP should align with user requirements. Different applications can accommodate different types of errors and uncertainties in the HRPPs. For example a drought analysis is interested in locations where little or no precipitation has fallen over long time intervals. A flood warning system needs to know how much rainfall has fallen over a period time ranging from hours to weeks. A flash flood warning systems needs to know times and locations of precipitation extremes. Ebert et. al. (2007) presented a summary of the over-land validation of 12 HRPPs and four NWP models done on a daily time scale and at a 25-km spatial resolution, summarized in Figure 2. This figure shows box-and-whiskers style comparisons of bias, equitable threat score (ETS), probability of detection (POD) and false alarm rate (FAR) amongst the HRPPs (colored boxes) and models (grayshade boxes). The left side of Figure 2 is for the region north of 30S latitude (predominantly tropical, convective rain), and the right side is for the region south of 30S latitude (mainly frontal based rain with more stratiform precipitation than convective). The main conclusions showed that HRPP-derived occurrence and amount are more accurate than NWP models during summer months and lower latitudes (mainly convective type precipitation). Conversely, NWP models exhibit superior performance compared to HRPPs during winter months and higher latitudes (mainly lighter, stratiform precipitation).

In order produce an assessment of the state of the error in various HRPPs, the first workshop of the Program for the Evaluation of High Resolution Precipitation Products (PEHRPP) was convened at the World Meteorological Organization (WMO) headquarters in December 2007 (Turk et, al, 2008). In this manuscript, we assess the performance of one HRPP (the NRL-Blend) over the central United States using both traditional gridded raingauge validation and also a non-traditional analysis using a land surface model (LSM). The LSM is forced using various precipitation datasets from the NRL-Blend, each simulating a proxy GPM satellite constellation, as described below.

## GROUND VALIDATION

In order to examine the impact of particular satellite types, nodal crossing times and sensor types (conical or crosstrack), the NRL-Blend technique (Turk and Miller, 2006) was configured for ten parallel runs, each mode employing different combinations of satellites and sensor types, beginning in June 2007. The NRL-Blend can be configured to run with any or all of a number of low Earth orbiting satellites with precipitation-sensing capabilities (specifically, an algorithm to estimate instantaneous rainrate from a combination of channels). Each of these runs employed a different set of satellites relative to the "all satellites" run. The all-satellites run, as the name suggests, utilized all 12 available low Earth-orbiting satellites for a total of 13 sensors: the crosstrack Advanced Microwave Sounding Units (AMSU) onboard the NOAA-15/16/17 satellites, the Microwave Humidity Sounder (MHS) onboard the NOAA-18 and METOP satellites, the Special Sensor Microwave Imagers (SSMI) onboard the Defense Meteorological Satellite Program (DMSP) F-13/14/15, the Special Sensor Microwave Imager Sounder (SSMIS) onboard F16/17, the Advanced Microwave Scanning Radiometer (ASMR-E) onboard Aqua, the WindSat onboard Coriolis, and the TRMM Microwave Imager (TMI) and companion Precipitation Radar (PR). All of these satellites orbit sun-synchronously with the exception of TRMM. NOAA-15/17, all DMSP, and Coriolis are in orbit patterns which crossover in mostly morning (AM) and evening (within a few hours of the solar terminator), whereas NOAA-16/18 and Aqua are in orbits which crossover in early afternoon (PM) and early morning (NOAA-16 is a backup and has drifted from its initial afternoon orbit crossing time). AMSU and MHS are across-track scanning sounders which can be used also for precipitation estimation, PR is an across-track scanning radar, whereas SSMI, SSMIS, WindSat and AMSR-E all scan conically.

As discussed below, the parallel runs of the NRL-Blend were configured to specifically study the impact of omitting either the morning (AM) or afternoon (PM) satellites, and the impact of omitting the crosstrack sounding instruments. The reasoning behind this is based on the fact that prior to and during the GPM era, the configuration of the microwave-capable satellite constellation is likely to change owing to program changes or launch schedule delays. Such changes could lead to the omission of certain key satellite/sensor systems, leading to the crosstrack sounders (designed mainly for temperature and humidity profiling and not precipitation sensing) being used for a larger role than originally envisioned in GPM. Sounding sensors such as AMSU and MHS are typically placed in AM or PM orbits to satisfy observation requirements for NWP data assimilation applications. Recent studies and algorithms have demonstrated that the AMSU channel suite, with its combined sounding and window channels, is capable of improved detection of precipitation at high latitudes (Surussavadee and Staelin, 2008). Therefore it is instructive to note how the performance of an HRPP (in this case, the NRL-Blend, but the concept could be extended to any HRPP) is affected by the loss of certain satellites at their associated nodal crossing times.

The ground truth data used is the optimal interpolation (OI) global daily gauge analysis provided by the National Oceanic and Atmospheric Administration (NOAA) Climate Prediction Center (CPC) (Chen et. al, 2008) over the continental United States during two 3-month periods, Jun-Aug 2007 (JJA) and Dec 2007-Feb 2008 (DJF).

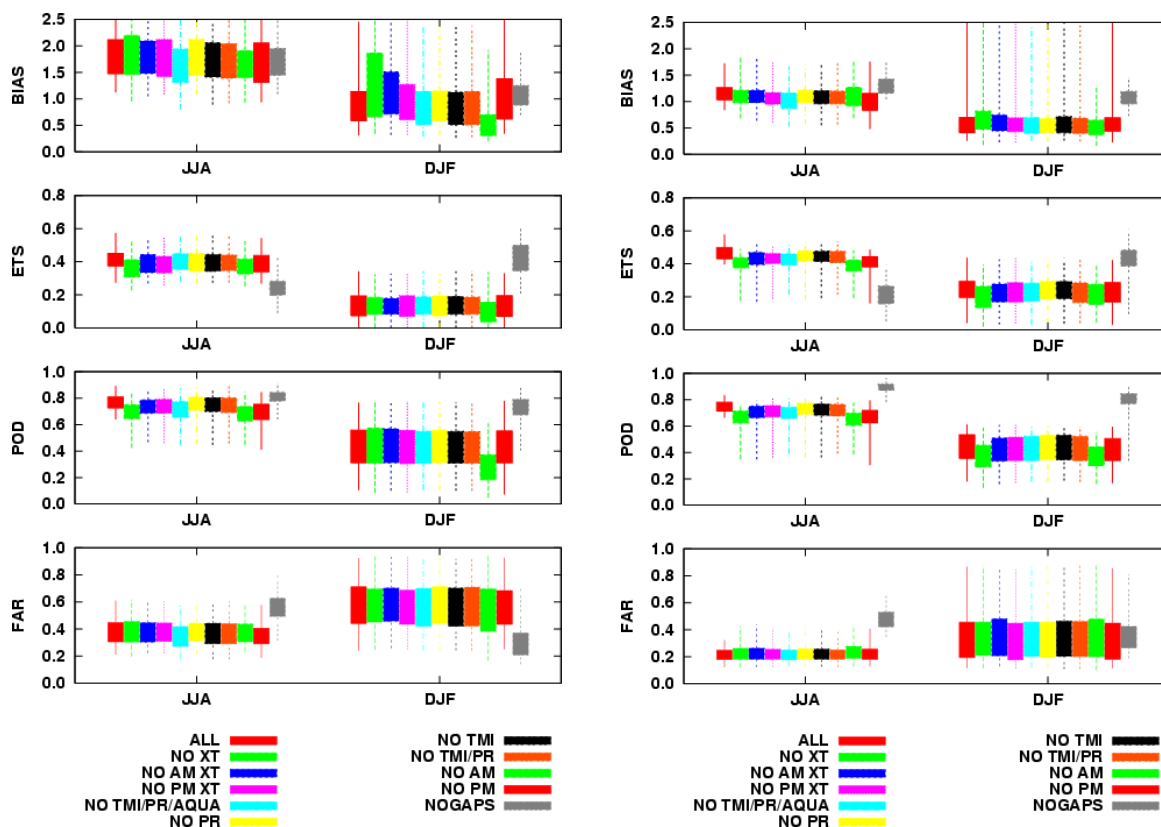


**Figure 3.** Seasonal performance of HRPP precipitation estimates using different satellite combinations over the continental United States west of 100 W longitude (left), and east of 100 W longitude (right), using a threshold of 1 mm day<sup>-1</sup>. From top, bias, equitable threat score (ETS), probability of detection (POD) and false alarm rate (FAR) from eight satellite-based HRPPs and four NWP models. Each color refers to a different set of satellites that was omitted from the “all satellites” baseline product from the NRL-Blend. “No XT” refers to no crosstrack sounders, “No AM XT” refers to no morning nodal crossing crosstrack sounders, “No TMI+PR+Aqua” refers to no TRMM TMI and PR and no AMSR-E from Aqua.

The panels in Figure 3 illustrate the performance using the identical box-and-whiskers type presentation as in Figure 2 and using the same 1 mm day<sup>-1</sup> threshold. The left figure only considers data west of 100W longitude (generally higher elevation terrain, colder surface backgrounds), and the right figure is for data east of 100W longitude. The colors refer to different runs of the NRL-Blend each with a different set of satellites. For example, “No AM XT” refers to the NRL-Blend precipitation estimates when all morning (time of ascending node near 1800 local) satellites with crosstrack sounders were omitted from the “all satellites” configuration of the NRL-Blend. “No PM XT” refers to the NRL-Blend precipitation estimates when all afternoon (time of ascending node near 1330 local) satellites with crosstrack sounders were omitted. Only one NWP model (NOGAPS) is shown (gray color). By intercomparing the bias, ETS, POD and FAR side-by-side, one can easily notice where one satellite combination performed better or worse than another, and how this ensemble of HRPPs performed relative to the NOGAPS model during summer and winter seasons, and at lower and higher elevations. In general, there is overall performance degradation for all HRPPs over the western United States (US) compared to the eastern US. This consistent with studies that have shown the poor performance of PMW scattering-based techniques when used over high elevation and complex terrain (Bennartz and Bauer, 2003). At first glance there is not much difference amongst the various satellite omission runs for the NRL-Blend “adjustment-based” HRPP technique, but closer inspection (green box) illustrates largest performance impact is the omission of the morning overpass crosstrack sounders (“No AM XT” and “No AM” configurations).

## LAND SURFACE MODEL VALIDATION

Impact and validation efforts also include the use of land surface models (LSM) and other types of hydrological observations (other than raingauge as was done above) to examine the impact of these GPM proxy data upon streamflow, discharge, soil moisture and other runoff measurements. By employing the Noah LSM (Ek et. al, 2003), incorporated with the NASA Land Information System (Kumar et. al, 2008), to simulate land surface and hydrological states, the performance impact of different GPM constellations can be examined. A similar methodology was used by Gottschalk et. al (2005). The analysis domain presented below covers the south-central United States where there are several well-instrumented watersheds in the Arkansas and Red River basins.

The impact of precipitation in a LSM is dependent upon many physical factors, such as soil type, vegetation, etc. and a soil moisture analysis at a given time is likely to be the cumulative result of precipitation that has fallen for weeks or months prior. To accommodate this, the results are shown after five months of simulation time, valid at 18 UTC on 31 October 2007. Soil moisture simulations are performed with  $0.1^\circ \times 0.1^\circ$  latitude-longitude resolution and the North American Land Data Assimilation System (NLDAS) forcing fields (except for precipitation) are used to run the Noah LSM from June through December 2007. Before performing these simulations, the Noah LSM was integrated for 2.5 years using the NLDAS atmospheric forcing only and initially homogeneous soil moisture (30% of vol. content) distribution in order to acquire "realistic" soil moisture fields. The colors in Figure 4 depict soil moisture difference relative to the "all-satellites" configuration, in the upper (0-10 cm) and deep layer (0.4-1 m).

While this single simulation time is interesting, these results are further substantiated by analyzing the histograms of the soil moisture difference (relative to "all-satellites" scenario) when plotted for an entire month. Figure 5 shows these results (each of the six panels uses a different constellation configuration, identical to Figure 4) for the entire month of October 2007, where daily average values of soil moisture were used to produce these histograms. Numbers in the upper right corners stand for mean difference of the soil moisture content in volumetric percent (white boxes indicate the 0-10 cm layer and black boxes indicate the 0.4-1 m layer). This mean difference can be considered as a typical bias of the soil moisture produced by the omission of the specific satellite and sensor. We note that the biggest impact (largest absolute values of the soil moisture biases of -0.46 % for the 0-10 cm layer and -0.52 % for the 0.4-1 m layer) is due to the omission of AM Satellites (Figure 5e) from the NRL-Blend. On the other hand, omission of PM satellites in the NRL-Blend resulted in the smallest impact upon the soil moisture simulated with the Noah model (Figure 5f). Although the relative magnitude of these changes is small, these results are consistent with the traditional raingauge-only validation shown in Figure 3.

Precipitation often has a predominant time-of-day cycle and therefore the local time of the observation is important. Relatively speaking, soil moisture changes over longer time scales than does precipitation. Therefore in the case of the soil moisture simulations, we note that the removal of the morning (AM) satellites likely has less to do with the specific local time-of-day observation than it does with the fact that the bulk of the current (2008) satellites such as DMSF, Coriolis and several NOAA have early morning crossing times. We note that these results are unique to the type of HRPP technique (NRL-Blend) used in this study, and the results may differ when used with other types of HRPP techniques.

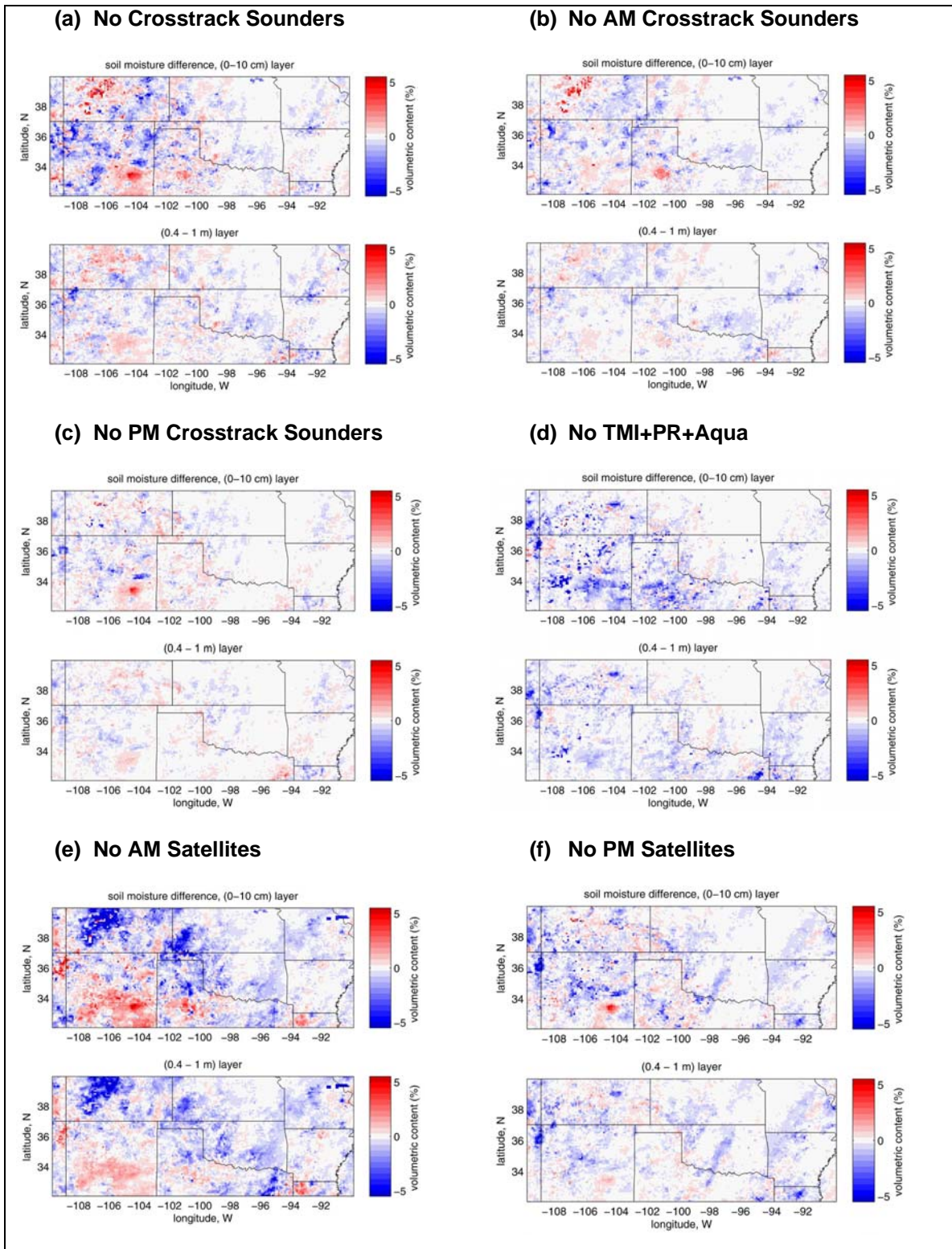


**Figure 4.** Soil moisture simulations performed with the Noah land surface model at a 0.1-degree resolution and using the North American Land Data Assimilation System (NLDAS) forcing fields (except for precipitation). These results are shown after five months of simulation time, valid at 18 UTC on 31 October 2007. The colors depict soil moisture difference relative to the all-satellites configuration in the upper (0–10 cm) and deep layer (0.4–1 m) for the six different GPM proxy constellations noted at the top of each panel.

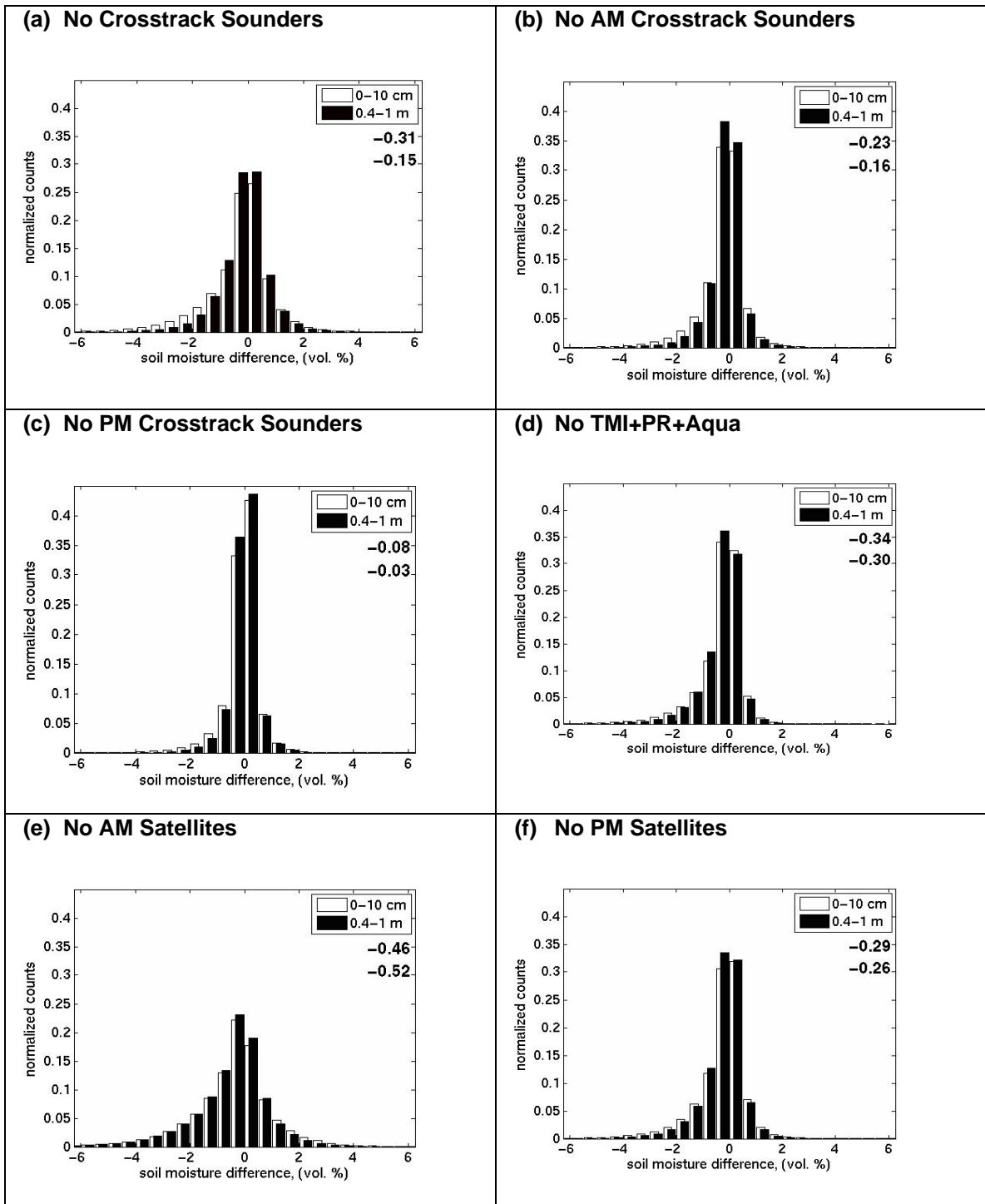


**Figure 5.** Same geographical domain as in Figure 4, where histograms of soil moisture difference relative to the all-satellites configuration in the upper (0-10 cm) and deep layer (0.4-1 m) for the six different GPM proxy constellations are shown. These results are for all data and simulations during October 2007.



## CONCLUSIONS

We have demonstrated the impact of omitting certain types of satellites and sensors upon the performance of a high resolution precipitation product (HRPP). The impact study was done using a raingauge analysis over the central United States, and also by examining the output of a land surface model (LSM) where the LSM was forced with different precipitation datasets. Each precipitation dataset corresponded to separate run of the NRL-Blend HRPP, where each run omitted one or more sensors relative to the “all satellites” satellite configuration. These omission experiments were designed to examine possible satellite constellation configurations that may exist during the GPM era.

While this example shows only one time step, these LSM simulations are being extended to cover the 2007-2008 calendar year, where the analysis can be broken into commonly-used three month periods. This extended analysis will help us to examine seasonal changes in modeled soil moisture when the LSM is driven by the different satellite constellations.

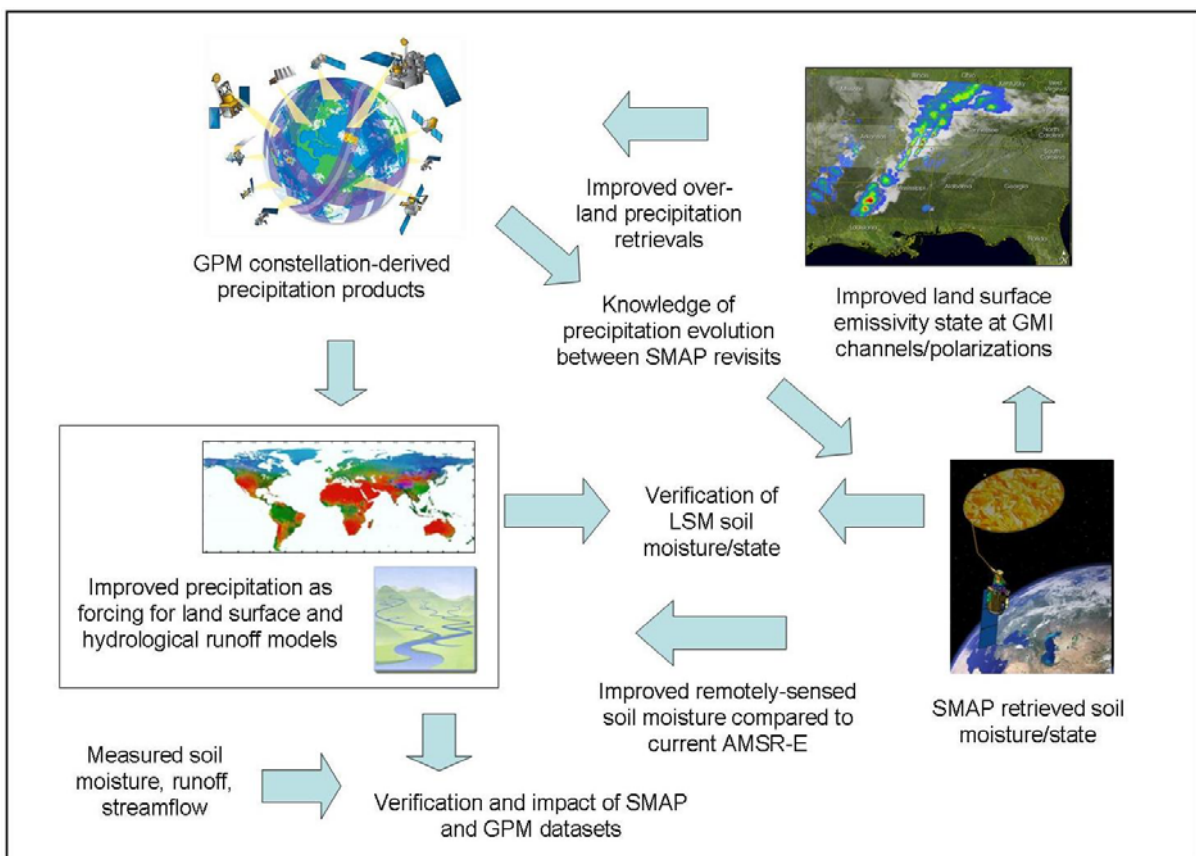


**Figure 6. Synergy between GPM and the Soil Moisture Active Passive (SMAP) mission.**

GPM is currently planned to be active during the NASA Soil Moisture Active Passive (SMAP) mission. There exists significant GPM-SMAP overlap in terms of science goals and applications, specifically towards the utilization of frequent precipitation estimates. The flowchart shown in Figure 6 shows several of these interconnections. For example, one of the biggest obstacles to improved over-land precipitation estimation is the large variability in land surface emissivity, which forms the “background” for passive microwave radiometric-based retrievals. The land surface microwave surface emissivity decreases with increased near-surface soil moisture, which in turn is related to the recent (hours to days) and longer (months and longer) accumulated precipitation. Conversely, GPM can potentially benefit SMAP soil moisture retrievals with its capability for improved tracking of precipitation evolution between SMAP revisits. The knowledge of where and how much precipitation occurred during

sequential SMAP revisits may benefit the soil moisture retrievals. Nevertheless, it is constructive to examine the connection between the missions at this early stage (when the science goals and user requirements are being formulated) so as to maximize the utility of these data towards achieving mission goals.

## REFERENCES

Bennartz, R. and P. Bauer, 2003: Sensitivity of microwave radiances at 85–183 GHz to precipitating ice particles. *Radio Science*, **38**, 4, 8075, doi:10.1029/2002RS002626.

Chen, M., W. Shi, P. Xie, V. B.S. Silva, V. Kousky, R. Higgins, J. Janowiak, 2008: Assessing objective techniques for gauge-based analyses of global daily precipitation. *J. Geophys. Res.*, **113**, D04110, 1-13.

Chen, F.W. and D.H. Staelin, 2003: AIRS/AMSU/HSB Precipitation Estimates, *IEEE Trans. Geosci. Rem. Sens.*, **41**, No. 2, 410-417.

Ebert, E., C. Kidd, J. Janowiak, 2007: Comparison of near real-time precipitation estimates from satellite observations and numerical models. *Bull. Amer. Meteor. Soc.*, **88**, 47-64.

Ek M. B., K. E. Mitchell, Y. Lin, E. Rogers, P. Grunmann, V. Koren, G. Gayno, and J. D. Tarpley, 2003: Implementation of Noah land surface model advances in the National Centers for Environmental Prediction operational mesoscale Eta model. *J. Geophys. Res.*, **108**, 8851, doi:10.1029/2002JD003296.

Gottschalck, J., J. Meng, M. Rodell, and P. Houser, 2005: Analysis of multiple precipitation products and preliminary assessment of their impact on Global Land Data Assimilation System land surface states. *J. Hydrometeor.*, **6**, 573–598.

Huffman, G.J., R.F. Adler, M. Morrissey, D.T. Bolvin, S. Curtis, R. Joyce, B McGavock, J. Susskind, 2001: Global Precipitation at One-Degree Daily Resolution from Multi-Satellite Observations. *J. Hydrometeor.*, **2**, 36-50.

Hsu, K., X. Gao, S. Sorooshian, and H.V. Gupta, 1997: Precipitation estimation from remotely sensed information using artificial neural networks, *J. Appl. Meteor.*, **36**, 1176-1190.

Joyce, R. J., J. E. Janowiak, P. A. Arkin, and P. Xie, 2004: CMORPH: A method that produces global precipitation estimates from passive microwave and infrared data at high spatial and temporal resolution. *J. Hydromet.*, **5**, 487-503.

Kumar, S. V., C. D. Peters-Lidard, J. L. Eastman and W.-K. Tao, 2008. An integrated high-resolution hydrometeorological modeling testbed using LIS and WRF. *Environmental Modelling & Software*, **23**, 169-181.

Surussavadee, C. and D. H. Staelin, 2008: Rain and snowfall retrievals at high latitudes using millimeter wavelengths, *Proc IGARSS 2008*, 6-11 July, Boston.

Turk, F.J and S. Miller, 2005: Toward improving estimates of remotely-sensed precipitation with MODIS/AMSR-E blended data techniques. *IEEE Trans. Geosci. Rem. Sens.*, **43**, 1059-1069.

Turk, F.J., P. Arkin, M. Sapiano, E. Ebert, 2008: Evaluating High Resolution Precipitation Products. To appear in *Bull. Amer. Meteor. Soc.*, December issue.